AD 631494

AD

USAAVLABS TECHNICAL REPORT 66-13

DERIVATION OF ROTOR BLADE GENERALIZED AIR LOADS FROM MEASURED FLAPWISE BENDING MOMENT AND MEASURED PRESSURE DISTRIBUTIONS

By

F. A. DuWaldt
I. C. Statler

CLEARINGHOUSE
FOR FEDERAL SCIENTIFIC AND
TECHNICAL INFORMATION
Hardcopy | Microfiche
5.60 | 0.75 | 60 pp as
ARCHIVE COPY
Code 1

March 1966

U. S. ARMY AVIATION MATERIEL LABORATORIES
FORT EUSTIS, VIRGINIA

CONTRACT DA 44-177-AMC-198(T)
CORNELL AERONAUTICAL LABORATORY, INC.
BUFFALO, NEW YORK

Distribution of this document is unlimited.

DISCLAIMERS

The findings in this report are not to be construed as an official Department of the Army position unless so designated by other authorized documents.

When Government drawings, specifications, or other data are used for any purpose other than in connection with a definitely related Government procurement operation, the United States Government thereby incurs no responsibility nor any obligation whatsoever; and the fact that the Government may have formulated, furnished, or in any way supplied the said drawings, specifications, or other data is not to be regarded by implication or otherwise as in any manner licensing the holder or any other person or corporation, or conveying any rights or permission, to manufacture, use, or sell any patented invention that may in any way be related thereto.

Trade names cited in this report do not constitute an official endorsement or approval of the use of such commercial hardware or software.

DISPOSITION INSTRUCTIONS

Destroy this report when no longer needed. Do not return it to originator.

DEPARTMENT OF THE ARMY
U. S. ARMY AVIATION MATERIEL LABORATORIES
FORT EUSTIS, VIRGINIA 23604

This report has been reviewed by the U. S. Army Aviation Materiel Laboratories. The results and conclusions are considered to be technically sound. The report is published for the exchange of information and the stimulation of ideas.

Task 1P125901A14229
Contract DA 44-177-AMC-198(T)
USAAVLABS Technical Report 66-13
March 1966

DERIVATION OF ROTOR BLADE GENERALIZED AIR LOADS FROM MEASURED FLAPWISE BENDING MOMENT AND MEASURED PRESSURE DISTRIBUTIONS

CAL Report BB-1959-S-1
by

F. A. DuWaldt
I. C. Statler

Distribution of this document is unlimited.

Prepared by

Cornell Aeronautical Laboratory, Inc.
Buffalo, New York

for

U. S. ARMY AVIATION MATERIEL LABORATORIES
FORT EUSTIS, VIRGINIA

SUMMARY

A limited study of methods of deducing generalized air loads acting on a helicopter rotor blade or a propeller blade from bending-moment measurements is presented. A new set of basic functions cal' d "orthonormal-moment distributions" is proposed as the best set for fitting the moment data.

The blade-tip deflections computed from pressure distributions measured on an H-34 helicopter rotor in steady level flight at 112 knots are compared with tip deflections derived by four methods based on use of measured bending-moment distributions. The degree of agreement between quantities obtained from the pressure distributions and those obtained from the moment distributions is encouraging but not satisfactory. Neither the lift nor the moment distributions were measured with sufficient accuracy for the purposes of the present study. Deficiencies in the accuracy of the measurements and in the accuracy of the description of the blade mass and elastic characteristics obscure any meaningful differences between the various methods of operating on the moment data.

FOREWORD

The work described in this report was conducted at the Cornell Aeronautical Laboratory, Inc. (CAL), for the U. S. Army Aviation Materiel Laboratories (USAAVLABS), Fort Eustis, Virginia, during the period from June 1964 through September 1965. The work was performed under Contract DA 44-177-AMC-198(T) and was administered by Mr. J. E. Yeates.

Mr. Frank A. DuWaldt and Dr. Irving C. Statler prepared this report; Mr. J. Kent performed most of the programming and computing tasks. Mr. Orren Tufts contributed to the analytical studies; Mr. Clarence Mesiah deserves special thanks for checking computer programs and carrying out numerous auxiliary calculations.

BLANK PAGE

CONTENTS

TABLES

SYMBOLS

a_o sectional lift curve slope

$C(r)$ blade chord, inches

d_i coefficient in series expansion (see equation 17)

$E(r)$ bending modulus of elasticity at station r, pounds per square inch

$G.A.$ generalized air load, pounds

$G_n(t)$ generalized force acting on n^{th} bending mode $\left(= \int_o^R t_a \phi_n dr\right)$ at time t, pounds

$I(r)$ structural area moment at station r, inches^4

K_n equivalent spring constant for n^{th} mode $\left(= \omega_n^2 \int_o^R m \phi_n^2 dr\right)$, pounds per inch

ℓ local lift, pounds per inch

$M_T(r)$ measured structural moment at station r, inch-pounds

$\hat{M}_{nk}$ maximum n^{th} mode bending moment for a unit generalized air load acting at frequency $k\Omega$, inch-pounds

$\mathcal{M}(r)$ natural mode moment at station r, inch-pounds

$\bar{\mathcal{M}}(r)$ orthogonal moment at station r, inch-pounds

$m(r)$ mass per unit spanwise length at station r, slugs per inch

$q(t)$ blade tip deflection at time t, inches

R blade radius, inches

r radial coordinate of blade measured from center of rotation, inches

t time, seconds

$t_a(r,t)$ part of aerodynamic load at station r and time t assumed independent of blade response, pounds per inch (see equation 29)

V forward flight velocity, inches per second

$\left(\frac{\overline{W}}{g}\right)_n$ equivalent mass $\left(=\int_0^R m(r)\,\phi_n^2\,dr\right)$, slugs

$y(r,t)$ bending deflection at station r and time t , inches

$y_k(r)$ bending deflection at station r at the frequency of the k^{th} harmonic of rotational speed $(y_k(r) \equiv y_{k_s}(r)\sin k\Omega t + y_{k_c}(r)\cos k\Omega t)$

ϵ_i error: difference between measured quantity and approximating series at station i

ϵ_k estimated error in k^{th} harmonic component of air load measurement, pounds per inch

Λ_k estimated threshold value of the k^{th} harmonic component of the air load measurement, pounds per inch

ξ dummy variable of integration

ρ density of air, pounds second^2 per inch^4

$\phi_n(r)$ normalized flapwise bending mode shape for n^{th} natural mode, inches per inch of tip deflection

Ω shaft rotational speed, radians per second

ω_n natural frequency for mode n , radians per second

ω frequency of oscillation, radians per second

ψ azimuthal angle, radians

Superscript.

derivative with respect to time: $\dot{f} \equiv \frac{df}{dt}$

Subscripts:

c cosine component of periodic function

k harmonic number = $\frac{\text{Frequency of oscillation}}{\text{Shaft rotational speed}} = \frac{\omega}{\Omega}$

m, n bending mode number

s sine component of periodic function

INTRODUCTION

Helicopter rotors and yawed propellers are subjected to oscillatory aerodynamic loads. These arise because of the periodicity of the tangential velocity when the actuator is yawed and because the wake, being unsymmetrical, introduces a nonuniform induced velocity distribution at the blading. Theoretically these oscillating loadings occur at all frequencies that are integral multiples of the rotational speed in the steady-state, yawed flight condition. These loads at the blading feed through to the control system and hub so that not only the blades but the linkages in the control system, the shafting, and the fuselage as well are all subjected continuously to periodic loadings. Design for a specified fatigue life obviously requires some knowledge of these oscillatory loads.

Few direct measurements of the aerodynamic forces acting on rotor or propeller blades exist, and only recently has appreciable progress been made in the development of theoretical techniques for predicting the higher-harmonic air loads. Consequently, blade designers have been forced to extrapolate past experience which, for the most part, has been based on interpretation of measured bending-moment distributions. Rational methods for interpreting flapwise bending-moment data in terms of the applied loads and for utilizing these in the analyses of similar configurations were developed. The rationale behind these methods is presented in References 1 and 2, and these expositions are highly recommended for both their technical and historical importance.

It was pointed out in Reference 1 that, if perfect bending-moment measurements were made and if the mass and elastic characteristics of the blade were known exactly, the spanwise aerodynamic load distribution could be obtained from measured structural strains to within the approximations of simple beam theory. The technique would involve the evaluation of differences of large numbers

and the double differentiation of these differences. As noted in Reference 1, the accuracy of such procedures could be expected to be poor, since the actual data are, in fact, inexact. It was believed that the combined errors resulting from measurement inaccuracies, approximations introduced in the data reduction, and the inherent inaccuracy of differentiating the experimental data would make the calculation of the aerodynamic loadings meaningless.

Since this direct attack on the problem was not feasible, several alternate techniques have been devised with the objective of minimizing at least those errors which are introduced in the data reduction procedures. These methods generally start from the assumption that the azimuthal variations of loads and bending moments are periodic. The bending-moment data are, therefore, harmonically analyzed and then the spanwise variation of each harmonic is assumed to be representable by the sum of a series of basic functions. These generic functions are so chosen as to "most likely" fit the measured data and to minimize the errors in the subsequent mathematical operations.

All of the analysis procedures which have previously been proposed used one or the other of two basic functions — either trigonometric or natural mode bending-moment distributions. Although, theoretically, an infinite number of terms is required to define perfectly the moment distributions, only a few seem to be needed in most practical cases and, in fact, the number is limited by the number of data points. Variations in the methods, therefore, generally involve only differences in the number of terms of the series which are retained in the representation.

The method which uses trigonometric functions as the basis is treated in detail in Reference 3. The measured moment data divided by the structural rigidity, EI, are fit with a truncated Fourier series whose double integral, according to simple beam theory, is the spanwise deflection curve. This curve can then be decomposed into a

linear combination of responses in the natural-mode shapes, taking advantage of the orthogonality of the natural modes. CAL has utilized this technique to calculate blade deflections for use in an aerodynamic force computation (Reference 4).

Approaches which use the natural-mode bending-moment distributions as basic functions are discussed in References 1, 2, and 5. There is a definite spanwise bending-moment distribution for each natural mode which can be obtained from beam vibration theory. If the transverse deflection of the blade, y_k, at the frequency of the k^{th} harmonic of rotational speed is represented by the following series in the natural mode shapes,

$$y_k(r) = \sum_{n=1}^{\infty} q_{nk}\, \phi_n(r),$$

then the corresponding bending-moment distribution is

$$M_{Tk}(r) = \sum_{n=1}^{\infty} q_{nk}\, m_n(r).$$

q_{nk} is the tip deflection due to bending in the n^{th} mode at the k^{th} harmonic of rotational frequency. The ϕ_n's and m_n's are considered to be known quantities determined by calculation or vibration tests.

A particularly simple variation of this approach uses only a single term of the series at each harmonic frequency. This technique is based on the assumption that the major response of the structure of the blade at each frequency is in the natural vibration mode nearest resonance with that frequency. All other modes are neglected, and the effects of interharmonic coupling for the particular mode are neglected. This single-mode approximation was justified on the basis of experimental observations and certain physical assumptions. It was further argued in Reference 2 that the available experimental data contained errors of the same order as those made in neglecting intermodal and interharmonic coupling. This approach is discussed in detail in References 1 and 2 and was used in the reduction of data reported in References 6 through 10.

Another variation which utilizes several terms of the series in normal-mode moment distributions rather than one, as in the preceding, is utilized in Reference 5. An improvement upon the single-mode approach is, in this case, represented by consideration of the first three bending modes at each harmonic frequency.

None of these techniques have proven to be particularly satisfactory. On the basis of physical arguments, the normal-mode moment distributions constitute a more satisfactory set of basic functions for representing the total moment than do the trigonometric functions. The neglect of the intermodal and interharmonic effects in the single-mode approximation seems too limited, but the complexity of the calculations increases rapidly as the number of modes considered is increased.

Recent events provided the impetus for initiating a new attack on the problem. Successful flight of helicopters in both pure and compound modes at relatively high advance ratios showed the existence of harmonic excitations at flight conditions that had been expected to benefit from the smoothing introduced by a large freestream velocity component through the rotor disc. A need for improved prediction of air loads was obvious.

A basis for a new approach resulted from the observation of Dr. H. Daughaday* of CAL that some of the errors introduced in reducing the data arose from the lack of orthogonality of the moment distributions in the normal modes. His suggestion that a set of orthogonal basic functions might be generated from the normal-mode moment distributions stimulated the development of the method reported here based on "orthonormal-moment distributions." The desirability of using orthogonal-moment distributions in reducing the data is based on theorems of linear algebra (see, e.g., Reference 11).

*Personal communication

All other considerations being equal, no other representation will be better than that in terms of orthonormal-moment distributions.

Perhaps the most significant event, however, was the in-flight simultaneous measurements of pressure distributions and structural moments on rotor blades in a series of programs initiated by the U. S. Army Aviation Materiel Laboratories at the National Aeronautics and Space Administration, the Bell Helicopter Corporation, and the Sikorsky Aircraft Corporation. These data provide, for the first time, the opportunity for comparing results obtained from moment distributions with those obtained from the measured pressure distributions. The various techniques for analyzing the bending-moment data might thereby be judged. The particular quantities compared in this report are the tip deflections in the normal modes and the generalized air loads as determined from the measured moment and pressure distributions.

To this end, the derivation of the modal tip deflections from the measured lift distributions is presented in the first section and the concept of a "generalized air load" is introduced. The second section contains a discussion of four techniques for converting measured bending moments to modal tip deflections. Values of tip deflections obtained by the various bending-moment data reduction schemes are compared with the corresponding results from pressure distributions in the third section. It is shown, however, that the comparison of the four techniques investigated is limited by the measurement accuracy of the available data. An evaluation of the moment measurement accuracy required to perform a meaningful judgment of these data reduction methods is, therefore, presented in the fourth section. There is also presented in this section a recapitulation of the measurement accuracy estimate given in the data report on the H-34 tests (Reference 12).

It should be recalled at this point that the objective of the studies reported in References 1, 2, and 5 was the development of a semiempirical method for estimating blade exciting forces for design purposes. Since the air-load distributions themselves cannot be determined accurately, the concept of the "generalized force," by means of which the effects of the aerodynamic loads on the bending moments might be approximated, is described in References 1, 2, and 5. The generalized forces, as developed in these references, follow directly from the modal tip deflections. This development and the important assumptions upon which it is based are reviewed in the fifth section. Generalized forces, as defined, do not include the aerodynamic forces that arise from bending deformations and are discussed in relation to the "generalized air loads" which include the aerodynamic damping, intermodal, and interharmonic forces.

1. THE DETERMINATION OF MODAL TIP DEFLECTIONS AND GENERALIZED AIR LOADS FROM MEASURED LIFT DISTRIBUTIONS

The linearized differential equation expressing the equilibrium of transverse forces on a helicopter rotor blade which is representable by a simple beam rotating at an angular velocity Ω is

$$\frac{\partial^2}{\partial r^2}\left(EI\frac{\partial^2 y}{\partial r^2}\right)+\Omega^2 r m\frac{\partial y}{\partial r}-\Omega^2\frac{\partial^2 y}{\partial r^2}\int_R^r m\xi\,d\xi+m\frac{\partial^2 y}{dt^2}=\mathscr{l}\left(r,t,\frac{\partial y}{\partial r},\frac{\partial y}{\partial t}\right). \quad (1)$$

The spanwise distribution of aerodynamic loading is represented by $\mathscr{l}$ and is a function of the radial position, r, the time, t, the blade spanwise bending slope, and the blade bending velocity. The bending deflection of the blade, y, is assumed to be representable by a double infinite series separable in r and t which reflects the periodicity of the loading and response in steady-state forward flight; namely,

$$y(r,t)=\sum_{n=1}^{\infty}\phi_n(r)\sum_{k=0}^{\infty}\left(q_{nk_c}\cos k\Omega t+q_{nk_s}\sin k\Omega t\right). \quad (2)$$

$\phi_n(r)$ is the mode shape corresponding to the n^{th} blade bending frequency, ω_n. Each of the bending-mode deflection shapes satisfies equation (1) with the aerodynamic loads set equal to zero, since removal of the aerodynamic terms reduces the equation to that for a vibrating beam in a vacuum. Equation (1) then becomes, for the mode at frequency ω_n,

$$\frac{\partial^2}{\partial r^2}\left(EI\frac{\partial^2\phi_n}{\partial r^2}\right)-\Omega^2\frac{\partial}{\partial r}\left[\frac{\partial\phi_n}{\partial r}\int_R^r m\xi\,d\xi\right]=m\omega_n^2\phi_n. \quad (3)$$

Substitution of equation (2) into equation (1) and introduction of equation (3) to simplify the results leads to the following equations for cosine and sine components:

$$\left.\begin{aligned}\sum_{n=1}^{\infty}\left(\omega_n^2 - k^2\Omega^2\right) m\phi_n q_{nk_c} &= \ell_{k_c} \\ \sum_{n=1}^{\infty}\left(\omega_n^2 - k^2\Omega^2\right) m\phi_n q_{nk_s} &= \ell_{k_s}\end{aligned}\right\} \qquad (4)$$

where the aerodynamic loading has been written as

$$\ell = \sum_{k=0}^{\infty} \ell_{k_c}\left(r, \frac{\partial y}{\partial r}, \frac{\partial y}{\partial t}\right) \cos k\Omega t + \sum_{k=0}^{\infty} \ell_{k_s}\left(r, \frac{\partial y}{\partial r}, \frac{\partial y}{\partial t}\right) \sin k\Omega t. \qquad (5)$$

Since the natural bending-mode shapes, ϕ_n, are orthogonal, the following relationship holds:

$$\int_0^R m(r)\,\phi_m(r)\,\phi_n(r)\,dr = 0 \qquad \text{for} \quad m \neq n .$$

Application of the principle of virtual work and the orthogonality condition permits the reduction of the cosine component, for example, of equation (4) to

$$\left(\omega_n^2 - k^2\Omega^2\right)\left(\frac{\bar{W}}{g}\right)_n q_{nk_c} = \int_0^R \ell_{k_c}\left(r, \frac{\partial y}{\partial r}, \frac{\partial y}{\partial t}\right)\phi_n(r)\,dr \equiv G.A._{nk_c} \qquad (6)$$

where $\left(\frac{\bar{W}}{g}\right)_n \equiv \int_0^R m\phi_n^2\,dr$ is the equivalent effective mass and q_{nk_c} is the cosine component of the tip deflection of the n^{th} mode at the k^{th} harmonic. $G.A._{nk_c}$ is defined as the integral over the span of the product of the n^{th} mode shape times the cosine component of the lift distribution, at frequency $k\Omega$, that would be derived from measured pressure distributions. This integral will be called the "generalized air load" and should not be confused with the integral historically described as the "generalized force." The differences in these two concepts are discussed in a later section of this report. For the present, it is sufficient to point out that the generalized force does not account for that part of the aerodynamic loading which is dependent on the blade deformation.

From equation (6), the modal tip deflections are proportional to the generalized air loads in accordance with

$$q_{nk_c} = \frac{G.A._{nk_c}}{\left(\omega_n^2 - k^2\Omega^2\right)\left(\frac{\bar{W}}{g}\right)_n} \cdot \tag{7}$$

2. THE DETERMINATION OF MODAL TIP DEFLECTIONS FROM MEASURED BENDING-MOMENT DISTRIBUTIONS

Direct measurement of blade motions by photographic means would be one possible method for obtaining tip deflections from which air load information might be derived. Generally, however, it is simpler to measure bending-moment distributions by means of strain gages bonded to the blade surface. The conversion of such bending-moment measurements to modal tip deflections is the subject of this section. This problem is essentially one of curve fitting, and it is from this general point of view that the four methods described herein are related. In the following discussion these four techniques are called (1) Total-Deflection Method, (2) Single-Mode Method, (3) Multi-Mode Method, and (4) Orthonormal-Moment Method.

The general technique is to expand the measured moment distributions (or functions of the moment distributions) in an assumed series, to evaluate the coefficients, and to deduce deflections. The mechanics of the operations are sketched in the discussion below. Details of the previously employed methods can be found in References 1, 2, 3, and 5.

The four techniques to be discussed differ in one or more of the following characteristics: (1) the quantity fitted; (2) the basis used, i.e., the functions used to fit the quantity: and (3) the dimension of the basis, i.e., the number of terms retained in the expansion. As pointed out in the Introduction, in each method the spanwise variation of the bending moment is represented by the sum of a series of basic functions. The methods to be compared utilize as basic functions either trigonometric functions, normal-mode bending-moment distributions, or orthonormal bending-moment distributions. The first of these is used in the approach which will be called the "Total Deflection" method.

According to simple-beam theory, $\frac{M(i)}{EI(i)}$ is the beam curvature at station i and its spanwise variation can be represented by a Fourier sine series such that the end conditions of zero moment at the root and tip for a pinned-free beam (the case of interest here) are satisfied. This series is integrated twice at each azimuthal position (the number of azimuthal positions being governed by the frequency range of interest), and two constants of integration appear at each position. The first of these is evaluated by equating $\left.\frac{dy}{dr}\right|_{r=0}$ to the measured root flapwise slope, and the second constant of integration is zero to satisfy the condition of zero displacement, $y|_{r=0}=0$, at the root. The resulting deflection shapes, $y(r,\psi)$, are decomposed into modal contributions at each azimuthal station, ψ_p , by a curve-fitting process; that is, the derived deflection shape at each ψ_p is represented by a finite series in which the natural-mode deflection shapes, $\phi_n(r)$, having unit tip deflections are generic functions. The deflection shape is represented by

$$y(r,\psi_p) = \sum_{n=1}^{\infty} q_n(\psi_p)\,\phi_n(r) \tag{8}$$

where the $\phi_n(r)$ are known from calculations or vibration tests and the coefficients, $q_n(\psi_p)$, are the modal tip deflections. The mode shapes weighted by the square root of the mass per unit span are orthogonal; i.e.,

$$\int_0^R m(r)\,\phi_m(r)\,\phi_n(r)\,dr = 0 \ , \qquad m \neq n$$

so that equation (8) can be solved for the tip deflections:

$$q_n(\psi_p) = \frac{\int_0^R y(r,\psi_p)\,m(r)\,\phi_n(r)\,dr}{\int_0^R m(r)\,\phi_n^2(r)\,dr} \ . \tag{9}$$

Under the assumption of periodicity in the azimuthal direction, expansion of q_n in a Fourier series in ψ yields the harmonic components of the tip deflections:

$$\left.\begin{aligned} q_{nk_c} &= \frac{1}{2\pi}\int_0^{2\pi} q_n(\psi)\cos k\psi\, d\psi \\ q_{nk_s} &= \frac{1}{2\pi}\int_0^{2\pi} q_n(\psi)\sin k\psi\, d\psi \end{aligned}\right\} \qquad (10)$$

In both the second and third methods, the bending moment data are first harmonically analyzed with respect to the azimuthal variation. The spanwise bending-moment distribution at each harmonic frequency, $k\Omega$, is then represented by the sum of a series of normal-mode bending-moment distributions:

$$M_{T_k}(r) = \sum_{n=1}^{\infty} q_{nk}\, m_n(r) \qquad (11)$$

where the $m_n(r)$ are known from calculations or vibration tests.

In the approach called the "Single-Mode" method, it is assumed that all the bending response occurs in a single natural bending mode — that estimated to be near resonance at the frequency in question. Consequently, the measured moment distribution is approximated by one term of the series with natural-mode moments as a basis [equation (11)]. In effect, the spanwise variation of the moment at each harmonic frequency is assumed a priori, and only the amplitude of that shape remains to be specified. If the natural-mode moments are defined for a unit tip deflection, then the coefficient, to be determined, of the natural-mode moment distribution is the tip deflection. In equation form,

$$M_{T_k}(r) \approx q_{n'k}\, m_{n'}(r)$$

or

$$q_{n'k_c} \approx \frac{M_{T_{k_c}}(r)}{m_{n'_c}(r)}$$

$$q_{n'k_s} \approx \frac{M_{T_{k_s}}(r)}{m_{n'_s}(r)} \cdot \qquad (12)$$

The subscript n' denotes the particular natural mode whose resonance is nearest the harmonic frequency, $k\Omega$, being considered.

The approach called the "Multi-Mode" method also proceeds from an expansion of the moment distribution in a series with $m_n(r)$ as the basis and coefficients q_{nk}. In this case, however, several terms of the series are retained; for example,

$$M_{T_k}(r) \approx \sum_{n=1}^{N} q_{nk}\, m_n(r).$$

The dimension N is selected such that the natural frequencies of the N modes completely span the frequency band up to the highest harmonic of shaft rotational speed of interest. For example, if the highest harmonic to be considered is the tenth, the dimension can be chosen as four since, generally, the first three flapwise bending modes have natural frequencies less than the tenth harmonic and the fourth mode frequency is not far above it. Of course, N can be no greater than the number of valid measurements of moment over the span.

The new technique developed in the current study is called the "Orthonormal-Moment" method. This approach differs from the Single-Mode and Multi-Mode methods only in the basic function which is used in the approximating series of equation (11). In all other respects, the procedures for determining the modal tip deflections are similar in these three methods. A new orthogonal set of basic functions, $\bar{m}_n(r)$, is derived from the natural-mode moment distributions.

The desirability of using orthogonal moment distributions in fitting the measured moment data is based on the theorems of linear algebra (see, e.g., Reference 11). Consider the measured moment distribution to be a vector, M_T, and the normal-mode moment distributions, m_i, to be linearly independent vectors in a linear manifold belonging to the same space as the measured moment. Then construct an orthonormal set of vectors, $\bar{m}_i$, which span the same linear manifold as the m_i. The vector

$$M_{T_p}(r) = \sum_{i=1}^{N} \left[\int_0^R M_T(\xi)\, \bar{m}_i(\xi)\, d\xi \right] \bar{m}_i(r) \tag{13}$$

is the projection of M_T on the manifold containing the m_i and $\bar{m}_i$ and is, of all vectors in the manifold, the nearest to M_T.

While the normal-mode shapes, ϕ_n, form an orthogonal set, the corresponding moment distributions, m_i, in general, do not, since the EI distribution is typically not constant across the span of a rotor blade. It is possible, however, to construct an orthonormal set of moments from the natural-mode moments by the Gram-Schmidt process (see, e.g., Reference 11). A vector of the set to be converted (i.e., an m_i) is chosen as the starting point and the first orthonormal vector is constructed. In the present case, the moment distribution, m_1, for the first pinned-free mode is a convenient starting point, and the first orthonormal function is

$$\bar{m}_1(r) = \frac{m_1(r)}{\sqrt{\int_0^R m_1^2(\xi)\, d\xi}} \,. \tag{14}$$

The second orthonormal function is constructed from the second-mode moment distribution, m_2, a correction term to make $\bar{m}_2$ perpendicular to m_1, and a normalizing divisor,

$$\bar{m}_2(r) = \frac{m_2(r) - \bar{m}_1(r)\int_0^R \bar{m}_1(\xi)\, m_2(\xi)\, d\xi}{\sqrt{\int_0^R \left[m_2(x) - \bar{m}_1(x)\int_0^R \bar{m}_1(\xi)\, m_2(\xi)\, d\xi\right]^2 dx}} \cdot \qquad (15)$$

This process is continued, each function $\bar{m}(r)$ being made to depend on $m_2(r)$ and to be orthogonal to all prior $\bar{m}$. That is,

$$\int_0^R \bar{m}_i(r)\, \bar{m}_j(r)\, dr = \begin{cases} 1 , & i = j \\ 0 , & i \neq j \end{cases} . \qquad (16)$$

Now the measured moment distribution can be written as a series in the constructed functions:

$$M_T(r) = \sum_{i=1}^{\infty} a_i\, \bar{m}_i(r) . \qquad (17)$$

For a fixed, finite number of terms, there is no other series which would constitute a better fit to the moment measurements. The amplitude coefficients, a_i, can be obtained explicitly from the measurements as

$$a_i = \int_0^R M_T(r)\, \bar{m}_i(r)\, dr \qquad (18)$$

by taking advantage of the orthonormality of the $\bar{m}$ functions.

The d_i coefficients can be related directly to the tip deflections in the normal modes. Use of the associated matrix method (Reference 13) produces a distribution of moments corresponding to a unit tip deflection in the particular mode calculated. Therefore, the measured moment distribution can also be expanded in the (nonorthogonal) natural-mode moment distributions

$$M_T(r) = \sum_{j=1}^{\infty} q_j m_j(r) \tag{19}$$

where q_j is the tip deflection in the j^{th} mode. The identity of the moment in the two coordinate systems [equations (17) and (19)] can be written

$$\sum_{j=1}^{\infty} q_j m_j(r) = \sum_{j=1}^{\infty} d_j \bar{m}_j(r). \tag{20}$$

Now it is noted that, in the Gram-Schmidt process, the $\bar{m}$ functions are linear combinations of the m functions, so they can be expressed as

$$\bar{m}_i = \sum_{h=0}^{i} \frac{\partial \bar{m}_i}{\partial m_h} m_h$$

so that equation (20) can be written

$$\sum_{j=1}^{\infty} q_j m_j = \sum_{i=1}^{\infty} d_i \sum_{h=0}^{i} \frac{\partial m_i}{\partial m_h} m_h. \tag{21}$$

Rearrangement of the right-hand side yields the following convenient form:

$$\sum_{j=1}^{\infty} q_j m_j = \sum_{j=1}^{\infty} \left(\sum_{i=j}^{\infty} d_i \frac{\partial m_i}{\partial m_j} \right) m_j$$

and, by equating coefficients of m_j,

$$q_j = \sum_{i=j}^{\infty} d_i \frac{\partial m_i}{\partial m_j}. \tag{22}$$

The α_i's are evaluated by equation (18) and the $\frac{\partial \bar{m}_i}{\partial m_j}$ from the construction of the orthonormal functions as represented by equations such as (14) and (15). The latter quantities, $\frac{\partial \bar{m}_i}{\partial m_j}$, can be evaluated as accurately as desired, depending on the number of stations at which the normal-mode bending moments are evaluated or measured.

In all but the Single-Mode method, there is a choice to be made of the number of terms to retain of a particular series representation. As pointed out previously, the number can never be greater than is consistent with the number of valid measurements. If the dimension of the basis selected is equal to the number of measurement points, the coefficients in the approximating function can be determined by requiring that the approximating function pass through the measured values. If the dimension is less than the number of measurement points, the coefficients in general cannot be so chosen. In view of the desire to minimize the number of terms of the series retained, it is this latter case that is of particular practical interest here. The difference between the measurement at station i and the approximating function at station i is defined to be the error, ε_i ; i.e.,

$$\varepsilon_i = \left[F(i) - f(i)\right]$$

where

$F(i)$ is the value to be fitted at the i^{th} station,

$f(i)$ is the value of the approximating series at the i^{th} station.

Generally, some criterion related to the error is used to permit evaluation of the coefficients of the base vectors in the approximating function $f(i)$. In fact, minimization of the sum of the squares of the errors was used as the criterion in all four techniques in this study.

In the Total-Deflection method, the least-square-error criterion is applied to the fitting of the generated deflection shape by the sum of a few normal-mode shapes, whereas the bending-moment measurements themselves are approximated in the other three methods.

In the Single-Mode method, the error is defined as

$$\varepsilon_{k_i} = M_{T_k}(i) - q_{n'k}\, m_{n'}(i),$$

and minimization of the sum of the squares of these errors results in the following equation for the tip deflection:

$$q_{n'k} = \frac{\sum_{i=1}^{P} M_{T_k}(i)\, m_{n'}(i)}{\sum_{i=1}^{P} \left[m_{n'}(i)\right]^2} \tag{23}$$

where P is the number of spanwise measurement stations.

The error in the Multi-Mode method is defined as

$$\varepsilon_{k_i} = M_{T_k}(i) - \sum_{n=1}^{N} q_{nk}\, m_n(i)$$

where N is the number of normal modes to be considered and is less than P. Minimization of the sum of the squared error produces N inhomogeneous equations from which the tip deflections are determined.

$$\begin{bmatrix} \sum_{i=1}^{P} \left[m_1(i)_2\right]^2 & \sum_{i=1}^{P} m_1(i) m_2(i) & \cdots & \sum_{i=1}^{P} m_1(i) m_N(i) \\ \sum_{i=1}^{P} m_1(i) m_2(i) & \sum_{i=1}^{P} \left[m_2(i)\right]^2 & \cdots & \sum_{i=1}^{P} m_2(i) m_N(i) \\ \vdots & \vdots & & \vdots \\ \sum_{i=1}^{P} m_1(i) m_N(i) & \sum_{i=1}^{P} m_2(i) m_N(i) & \cdots & \sum_{i=1}^{P} \left[m_N(i)\right]^2 \end{bmatrix} \begin{bmatrix} q_{1k} \\ q_{2k} \\ \vdots \\ q_{Nk} \end{bmatrix} = \begin{bmatrix} \sum_{i=1}^{P} M_{T_k}(i) m_1(i) \\ \sum_{i=1}^{P} M_{T_k}(i) m_2(i) \\ \vdots \\ \sum_{i=1}^{P} M_{T_k}(i) m_N(i) \end{bmatrix} \tag{24}$$

This operation can be considerably simplified in the Orthonormal-Moment method. As in the Multi-Mode method, the error is

$$\varepsilon_{k_i} = M_{T_k}(i) - \sum_{n=1}^{N} \alpha_{nk}(i)\, \bar{m}_n(i)$$

and the coefficients α_{nk} are determined such that the sum of the squares of these errors is minimized. The set of equations for these coefficients is similar to that in equation (24). If the measurement

stations are nearly equally spaced, however, the following simplification can be introduced as a consequence of the orthogonality of the functions $\bar{m}_n$:

$$\sum_{i=1}^{P} \bar{m}_m(i)\, m_n(i) \approx \text{constant} \cdot \int_0^R \bar{m}_m(r)\, m_n(r)\, dr = \begin{cases} 0 & ; \ m \neq n \\ \text{constant} & ; \ m = n \end{cases}.$$

The equations for the d_{nk} then become simply

$$d_{nk} = \frac{\sum_{i=1}^{P} M_{T_k}(i)\, m_n(i)}{\sum_{i=1}^{P} [\bar{m}_n]^2} . \tag{25}$$

The coefficients are related to the normal-mode tip deflections by equation (22). The above factors are summarized in Table I.

TABLE I

SUMMARY OF CHARACTERISTICS OF METHODS FOR FITTING MOMENT DATA

METHOD	QUANTITY FITTED	BASIC FUNCTION	DIMENSION	ERROR CRITERION
"TOTAL DEFLECTION"	$y(r) = \iint \frac{M_T}{EI} d\xi\, d\xi$	$\phi_n(r)$	DETERMINED BY NUMBER OF MODES HAVING NATURAL FREQUENCIES IN FREQUENCY RANGE OF INTEREST.	MINIMUM $\Sigma \varepsilon_i^2$
"SINGLE MODE"	$M_{T_k}(i)$	$m_n(r)$	1	
"MULTIPLE MODE"	$M_{T_k}(i)$	$m_n(r)$	DETERMINED BY NUMBER OF MODES HAVING NATURAL FREQUENCIES IN FREQUENCY RANGE OF INTEREST.	
"ORTHONORMAL MOMENTS"	$M_{T_k}(i)$	$\bar{m}_n(r)$		

$M_{T_k}(i)$ = Measured moment at the k^{th} harmonic at station i.

$m_n(r)$ = Radial distribution of natural-mode moment per unit tip deflection.

$\bar{m}_n(r)$ = Radial distribution of constructed orthonormal moments.

$\frac{M_T}{EI} = \sum_{j=1}^{P} h_j \sin \frac{(2j-1)\pi r}{R}$; where P = number of measurement stations.

It is appropriate at this point of discussion to introduce a few comments with regard to consistent data processing. The least-square-error criterion, which has been used, weights all the measurement errors equally. Practical considerations of the actual measuring system, however, justify the intelligent filtering of these data prior to analysis. For example, very small moment amplitudes should probably be discarded on the basis of threshold limitations of the measuring system. Moment measurements which indicate discontinuities can usually also be discarded as being physically unrealistic. The minimum number of azimuthal measurement points that remains determines the highest harmonic that could possibly be considered; the minimum number of radial stations that remains determines the highest order of the normal or orthonormal mode in the spanwise representation. In addition to the threshold considerations, a further restriction results from the limits of overall accuracy of the measurement system. Any mode whose maximum amplitude is found to be less than the possible error due to measurement inaccuracy should properly be discarded.

These considerations were introduced in the treatment of the data used in the next two sections.

3. COMPARISON OF TIP DEFLECTIONS AND GENERALIZED AIR LOADS DERIVED FROM MEASURED LIFT DISTRIBUTIONS AND BENDING MOMENTS

It was pointed out in Section 1 that modal tip deflections can be obtained from the generalized air loads calculated from measured lift distributions. Methods for reducing measured bending-moment data to obtain modal tip deflections were discussed in Section 2. Numerical results based on Data Table 21 of Reference 12 are presented and discussed in this section.

The data from Table 21 of Reference 12 which were used in the present calculations are reproduced in Table II. The aerodynamic load distributions presented in part (b) of Table II were used to evaluate the generalized air loads for the first four natural bending modes. The results are presented in Table III. The smaller values indicated in Table III (that is, values less than about ten) are probably without meaning because of the errors in the measurement and the errors introduced in the integration. Errors in the integration arise because the spanwise distribution of measurement stations is such that curves drawn through the data points are not well defined. This can be seen in Figure 1 where the harmonic air load data are presented. The estimated accuracy of the values indicated in Table III is presented in Section 4 as part of an effort to establish corresponding bending-moment accuracy requirements.

The four analysis techniques described in Section 2 were applied to the bending-moment measurement data presented in part (a) of Table II.

Table IV contains a listing of the harmonics of modal tip deflections deduced from bending moments and from lift distributions. The deflections corresponding to the lift distributions are used as the standard in the following discussion. It can be noted immediately that

TABLE II

FLIGHT TEST DATA (REFERENCE 12)

FLIGHT 18, TRIM LEVEL FLIGHT OUT-OF-GROUND EFFECT (V = 112 KNOTS)

(a) Flapwise bending moment

ψ_{norm}, deg	Flapwise bending moment, in-lb, at -							
	r/R = 0.150	r/R = 0.275	r/R = 0.375	r/R = 0.450	r/R = 0.575	r/R = 0.650	r/R = 0.800	r/R = 0.925
6	2378	2492	3137	2311	484	-2753	-6741	-6672
21	2359	3853	4647	3618	1461	-1699	-5701	-6076
36	3495	3655	4683	3990	2567	112	-3080	-4168
51	2845	2657	3381	2721	2438	739	-1062	-2635
66	1922	1526	1898	766	502	-1062	-1391	-2373
81	1796	462	136	-1152	-1971	-4017	-4231	-3110
96	1192	-314	-1003	-2821	-4171	-6425	-5680	-3227
111	611	-1188	-2061	-3699	-4725	-6813	-5591	-2789
126	-336	-1625	-2106	-3690	-4470	-6415	-4969	-2314
141	280	-1460	-1953	-3279	-3704	-5967	-5507	-2949
156	360	-957	-850	-2239	-3704	-6433	-6224	-3723
171	622	-586	-389	-1848	-3863	-6942	-7191	-4694
186	907	-256	-271	-1991	-4074	-6863	-7003	-4672
201	1477	347	-118	-2106	-3810	-6226	-6449	-4431
216	1682	1106	913	-999	-2675	-5251	-5920	-4190
231	2138	2203	2459	1080	-396	-2813	-4691	-3957
246	2560	3267	3842	2960	2042	252	-1893	-3146
261	1967	3762	4827	4010	4532	3406	1088	-1949
276	1728	3762	5080	5249	5896	5097	2427	-1759
291	2058	3655	4800	4706	5228	4500	2493	-1671
306	1944	2962	3842	3551	3864	2898	811	-2373
321	1010	1865	2676	2225	2218	759	-1736	-3964
336	941	1190	1826	1064	854	-1062	-3828	-5154
351	1317	1502	1989	966	0	-2345	-5141	-5869

(b) Section aerodynamic loading

ψ_{norm}, deg	Section aerodynamic loading, l, lb/in., at -						
	r/R = 0.25	r/R = 0.40	r/R = 0.55	r/R = 0.75	r/R = 0.85	r/R = 0.90	r/R = 0.95
6	.00	3.05	9.72	20.30	31.96	31.36	29.57
21	.41	4.92	11.58	22.03	31.00	30.10	28.41
36	2.52	6.51	11.84	22.26	26.98	25.87	24.78
51	2.06	6.40	10.43	18.31	20.95	19.87	19.71
66	1.84	5.41	8.22	14.44	16.11	14.82	16.37
81	1.80	4.83	6.87	11.01	12.46	11.23	13.70
96	2.73	5.42	6.95	8.75	9.70	8.19	10.21
111	4.17	7.53	9.20	8.63	8.32	5.63	6.91
126	5.97	10.23	11.90	11.39	10.53	6.73	7.39
141	7.74	12.20	14.02	15.02	13.56	9.86	9.78
156	9.14	12.83	15.14	17.77	18.16	14.75	14.05
171	8.76	12.42	17.46	20.14	22.36	19.48	17.76
186	6.77	10.67	17.78	20.96	24.30	21.74	19.67
201	3.30	7.32	14.03	18.85	23.53	21.46	19.51
216	.79	4.54	10.82	16.18	22.53	20.36	18.88
231	-.34	2.95	7.88	14.70	21.65	20.30	18.83
246	-1.77	1.90	5.57	13.19	21.07	20.69	19.36
261	-2.37	1.11	3.92	11.71	19.95	20.38	19.72
276	-2.20	1.01	2.76	10.51	19.42	20.08	20.49
291	-1.97	1.07	2.15	9.50	18.80	19.94	21.00
306	-1.26	1.53	2.49	9.34	18.75	19.79	21.18
321	-.69	1.97	3.73	11.62	22.07	23.51	24.41
336	.07	2.68	5.75	14.68	26.57	27.97	27.41
351	.25	2.61	7.92	18.00	29.78	30.22	29.28

TABLE II (Contd)

(c) Harmonic analysis of section aerodynamic loading

r/R	n	L_n, lb/in.	M_n, lb/in.	r/R	n	L_n, lb/in.	M_n, lb/in.	r/R	n	L_n, lb/in.	M_n, lb/in.
.25	0	1.988		.75	0	14.991		.95	0	19.099	
.25	1	-2.560	3.232	.75	1	.267	.875	.95	1	5.397	-4.864
.25	2	1.643	-1.542	.75	2	5.568	1.767	.95	2	4.838	1.305
.25	3	-.464	.852	.75	3	.094	1.730	.95	3	-.261	.455
.25	4	-.245	-.275	.75	4	.141	-.200	.95	4	.887	-.692
.25	5	-.235	.115	.75	5	-.239	-.021	.95	5	.060	.208
.25	6	-.125	-.228	.75	6	-.003	.079	.95	6	-.191	.169
.25	7	-.137	-.040	.75	7	-.286	-.015	.95	7	-.291	.122
.25	8	.021	-.092	.75	8	.093	-.069	.95	8	-.014	.024
.25	9	-.063	-.126	.75	9	.014	-.091	.95	9	.111	-.015
.25	10	.041	-.020	.75	10	.058	-.093	.95	10	-.014	-.046
.40	0	7.451		.85	0	20.438					
.40	1	-5.442	6.772	.85	1	3.425	-3.915				
.40	2	3.482	-2.814	.85	2	6.822	1.817				
.40	3	-.826	2.137	.85	3	.607	1.001				
.40	4	-.685	-.285	.85	4	.825	-.434				
.40	5	-.579	.114	.85	5	-.052	.136				
.40	6	-.143	-.262	.85	6	-.055	.059				
.40	7	-.313	-.021	.85	7	-.255	.182				
.40	8	.017	-.099	.85	8	.013	.016				
.40	9	-.107	-.126	.85	9	.127	.040				
.40	10	.041	-.005	.85	10	.016	-.015				
.55	0	9.089		.90	0	19.347					
.55	1	-3.066	3.367	.90	1	4.902	-5.440				
.55	2	4.207	.119	.90	2	6.372	1.799				
.55	3	-.117	1.104	.90	3	.261	.777				
.55	4	.154	.228	.90	4	.964	-.698				
.55	5	-.482	-.059	.90	5	-.196	.208				
.55	6	.202	-.074	.90	6	-.174	.093				
.55	7	-.215	.116	.90	7	-.306	.101				
.55	8	.069	-.114	.90	8	.020	.094				
.55	9	-.099	.066	.90	9	.145	.081				
.55	10	.041	-.051	.90	10	.009	-.005				

$$l = L_0 + \sum_{n=1}^{10} \left[L_n \cos n \left(\psi_{nom} - 6^o\right) + M_n \sin n \left(\psi_{nom} - 6^o\right) \right]$$

TABLE III

GENERALIZED AIR LOADS EVALUATED FROM MEASURED PRESSURE DISTRIBUTIONS

$$G.A._{nk} = \int_0^R \ell_k \left(r, \frac{\partial y}{\partial r}, \frac{\partial y}{\partial t} \right) \phi_n(r)\, dr \text{ , pounds}$$

HARMONIC ORDER, $k=\frac{\omega}{\Omega}$		MODE 1 $\frac{\omega_1}{\Omega}$ =2.72	MODE 2 $\frac{\omega_2}{\Omega}$ =4.95	MODE 3 $\frac{\omega_3}{\Omega}$ =7.84	MODE 4 $\frac{\omega_4}{\Omega}$ =13.1
1	COSINE	488.7	-110.3	-148.1	62.0
	SINE	-507.7	141.6	139.7	14.4
2	COSINE	-136.6	- 92.6	- 40.6	-73.9
	SINE	139.0	-167.3	- 57.2	35.5
3	COSINE	42.8	- 30.8	- 15.6	-19.4
	SINE	-103.8	10.2	2.4	-34.0
4	COSINE	47.5	- 21.0	- 12.5	- 6.4
	SINE	- 11.4	- 18.8	14.8	10.2
5	COSINE	37.2	- 3.1	- 11.6	4.7
	SINE	4.8	8.2	- 1.1	- 5.6
6	COSINE	- 1.3	- 12.4	3.7	3.0
	SINE	37.3	3.2	- 21.8	- 5.2
7	COSINE	13.0	- 4.1	- 1.6	9.4
	SINE	1.9	- 2.3	5.2	- 0.5
8	COSINE	- 0.7	- 1.7	- 1.6	- 1.3
	SINE	10.8	3.5	- 0.5	- 4.6
9	COSINE	4.6	0.7	- 2.4	- 2.6
	SINE	5.5	- 5.2	2.8	- 2.9
10	COSINE	- 0.8	- 0.4	- 1.0	- 0.7
	SINE	0.4	3.2	2.3	0

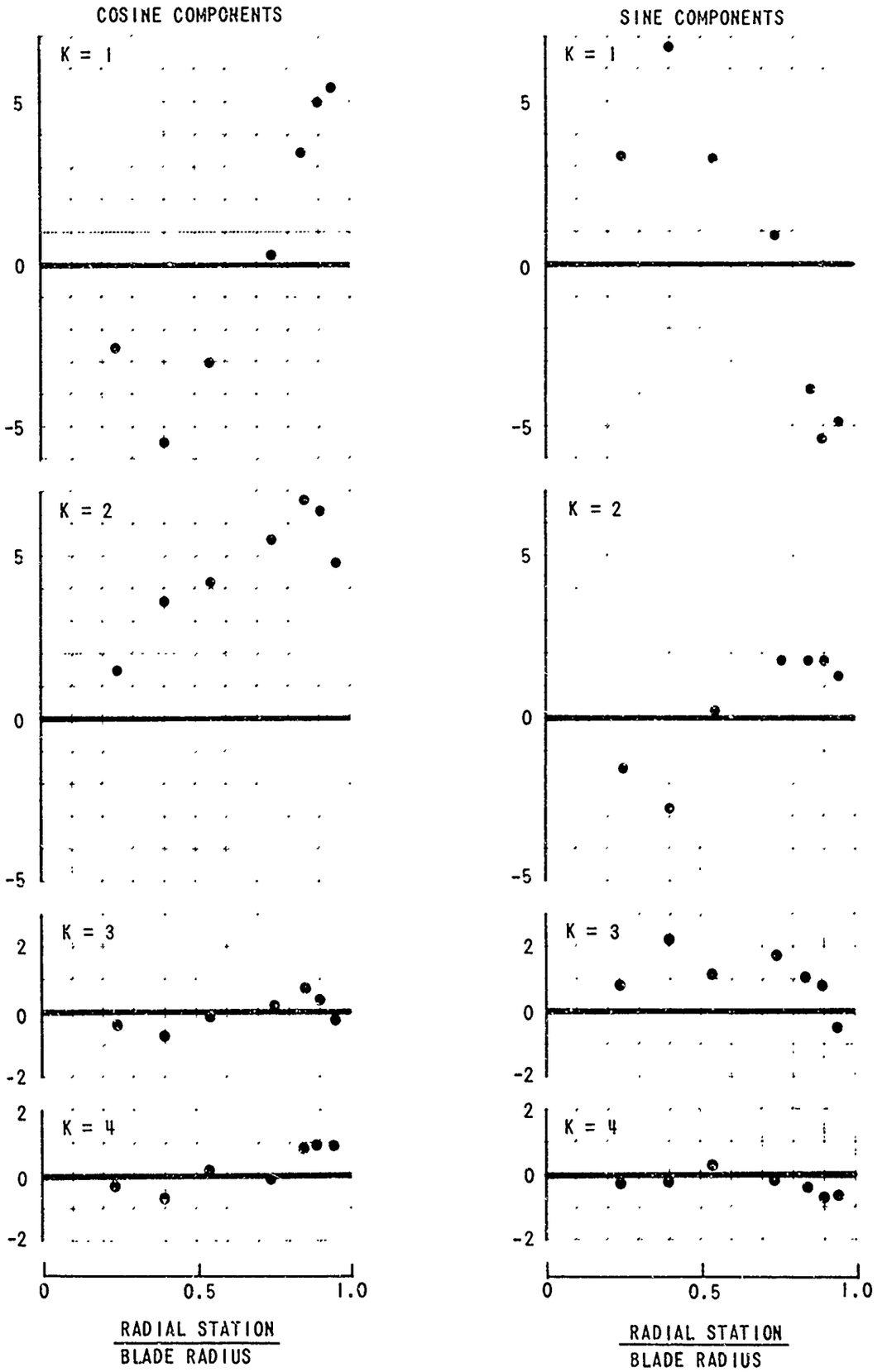

Figure 1 MEASURED HARMONIC LIFT DISTRIBUTIONS;
H-34, V = 112 KNOTS (DATA TABLE 21, REFERENCE 12)

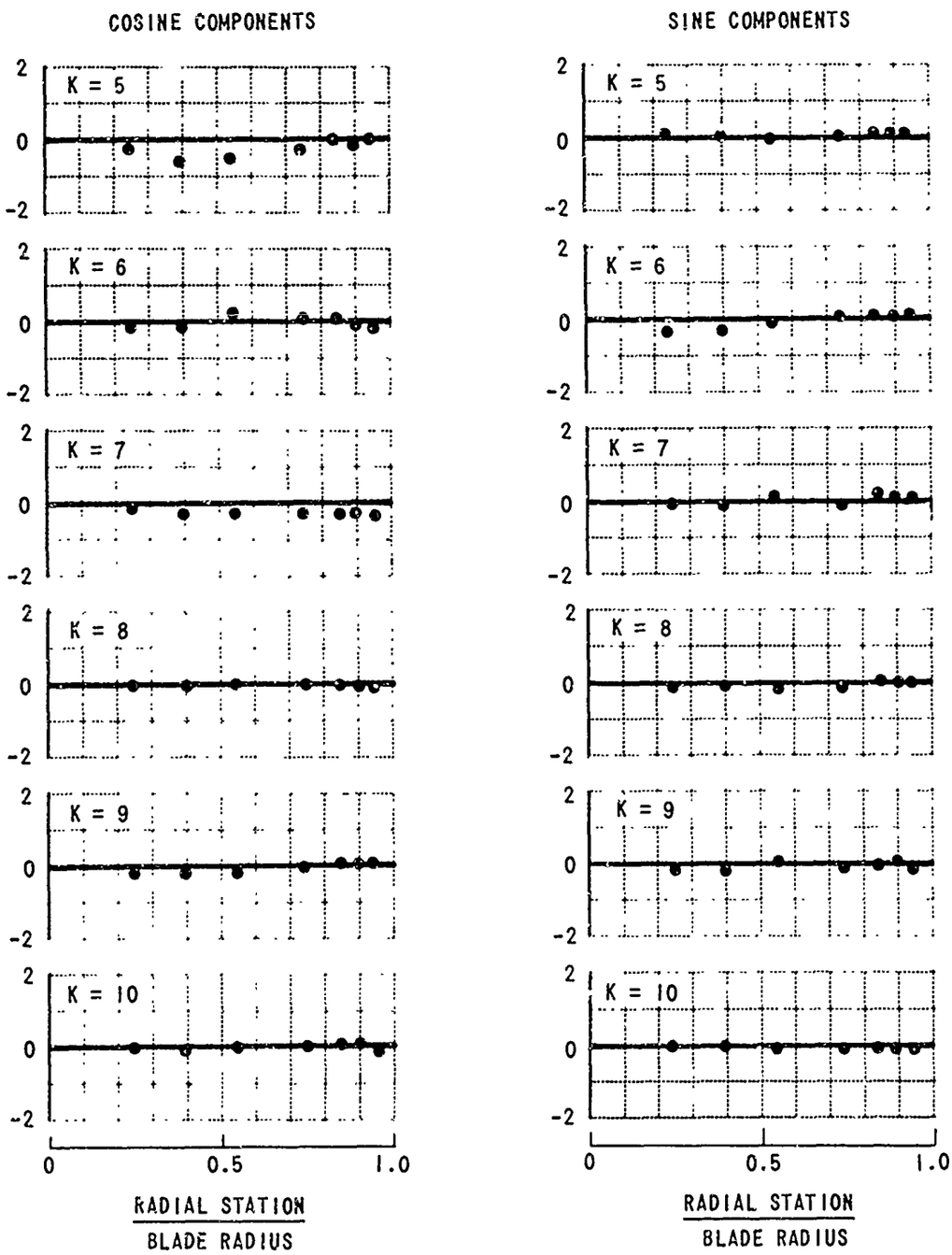

Figure I (Contd)

TABLE IV
COMPARISON OF DERIVED HARMONIC COMPONENTS OF MODAL TIP DEFLECTIONS

Method of Analysis	Harmonic Order $k = \frac{\omega}{\Omega}$	q_{1k} (inches)		q_{2k} (inches)		q_{3k} (inches)		q_{4k} (inches)	
		Cos	Sin	Cos	Sin	Cos	Sin	Cos	Sin
Air Load		1.6570	-1.7210	-0.0902	0.1160	-0.0410	0.0387	0.0062	0.0014
Total Deflection		1.7950	-1.6220	0.0035	-0.0164	0.0195	-0.0079	0.0441	-0.0750
Single Mode	1	1.5060	-1.7050	-	-	-	-	-	-
Multi Mode		1.5140	-1.7400	-0.0256	-0.0262	-0.0372	0.0349	-0.0113	0.0047
Ortho Moments		1.4800	-1.7350	-0.0252	-0.0342	-0.0370	0.0352	-0.0115	0.0048
Air Load		-0.8730	0.8800	-0.0868	-0.1570	-0.0118	-0.0167	-0.0075	0.0036
Total Deflection		-0.9150	0.5720	-0.1570	-0.1660	-0.0534	-0.0068	-0.1120	-0.0473
Single Mode	2	-0.5770	0.6620	-	-	-	-	-	-
Multi Mode		-0.6560	0.6290	-0.0936	-0.0842	0.0124	0.0049	0.0272	0.0022
Ortho Moments		-0.6520	0.6320	-0.0952	-0.0858	0.0136	0.0058	0.0274	0.0023
Air Load		-0.5770	1.3980	-0.0382	0.0126	-0.0049	0.0007	-0.0020	-0.0035
Total Deflection		-0.5890	0.9050	-0.0861	-0.0418	-0.0340	-0.0296	-0.0277	-0.0442
Single Mode	3	-0.2930	0.9620	-	-	-	-	-	-
Multi Mode		-0.2570	0.9630	-0.0585	0.0159	-0.0126	0.0070	-0.0005	0.0091
Ortho Moments		-0.2560	0.9640	-0.0588	0.0160	-0.0125	0.0071	-0.0005	0.0091
Air Load		-0.1200	0.0287	-0.0473	-0.0424	-0.0046	0.0054	-0.0007	0.0011
Total Deflection		-0.1900	0.0363	-0.0710	-0.0141	-0.0332	0.0246	-0.0199	0.0114
Single Mode	4	-	-	-0.0625	-0.0164	-	-	-	-
Multi Mode		-0.1430	-0.0244	-0.0526	-0.0082	-0.0025	0.0138	-0.0019	0.0052
Ortho Moments		-0.1440	-0.0274	-0.0524	-0.0089	-0.0027	0.0143	-0.0020	0.0052
Air Load		-0.0458	-0.0059	0.1360	-0.3550	-0.0051	-0.0005	0.0005	-0.0006
Total Deflection		-0.0179	-0.0118	0.0451	-0.0563	0.0199	0.0163	0.0009	0.0136
Single Mode	5	-	-	-0.0491	-0.0838	-	-	-	-
Multi Mode		-0.1498	-0.0233	-0.0333	-0.0839	0.0073	-0.0029	-0.0014	0.0003
Ortho Moments		-0.1499	-0.0237	-0.0331	-0.0836	0.0071	-0.0031	-0.0015	0.0003
Air Load		0.0010	-0.0283	0.0208	-0.0054	0.0024	-0.0144	0.0003	-0.0006
Total Deflection		0.0198	-0.0372	0.0354	-0.0362	0.0199	-0.0261	0.0119	-0.0175
Single Mode	6	-	-	-0.0209	-0.0097	-	-	-	-
Multi Mode		-0.0397	-0.0048	-0.0012	-0.0099	0.0080	-0.0019	-0.0021	-0.0009
Ortho Moments		-0.0996	-0.0049	-0.0012	-0.0099	0.0078	-0.0019	-0.0021	-0.0009
Air Load		-0.0067	-0.0010	0.0032	0.0018	-0.0021	0.0069	0.0013	-0.0001
Total Deflection		-0.0610	-0.0200	-0.0310	-0.0190	-0.0170	-0.0202	-0.0098	-0.0043
Single Mode	7	-	-	-	-	0.0006	-0.0112	-	-
Multi Mode		-0.0786	0.0386	-0.0022	-0.0038	0.0033	-0.0151	-0.0014	-0.0012
Ortho Moments		-0.0786	0.0382	-0.0023	-0.0038	0.0032	-0.0151	-0.0015	-0.0012
Air Load		0.0003	-0.0041	0.0008	-0.0017	0.0002	0.0031	-0.0002	-0.0007
Total Deflection		-0.0248	0.0547	-0.0103	0.0350	-0.0143	0.0232	-0.0026	0.0193
Single Mode	8	-	-	-	-	-0.0057	-0.0069	-	-
Multi Mode		-0.0481	0.0593	-0.0036	-0.0025	-0.0039	-0.0120	-0.0021	-0.0048
Ortho Moments		-0.0480	0.0588	-0.0037	-0.0075	-0.0039	-0.0121	-0.0021	-0.0048
Air Load		-0.0013	-0.0016	-0.0002	0.0018	0.0020	-0.0023	-0.0005	-0.0005
Total Deflection		0.0411	0.0175	0.0399	0.0064	0.0268	0.0032	0.0199	0.0076
Single Mode	9	-	-	-	-	-0.0048	-0.0081	-	-
Multi Mode		0.0096	0.0554	-0.0020	-0.0014	-0.0046	-0.0129	-0.0001	-0.0046
Ortho Moments		0.0096	0.0548	-0.0021	-0.0014	-0.0046	-0.0131	-0.0001	-0.0046
Air Load		0.0002	-0.0001	0.0001	-0.0006	0.0004	-0.0010	-0.0002	0.0000
Total Deflection		0.0084	-0.0519	0.0016	-0.0406	0.0016	-0.0313	-0.0010	-0.0172
Single Mode	10	-	-	-	-	-	-	0.0017	0.0001
Multi Mode		0.0600	0.0916	0.0024	-0.0062	-0.0029	-0.0134	0.0018	-0.0027
Ortho Moments		0.0598	0.0901	0.0025	-0.0058	-0.0028	-0.0137	0.0018	-0.0028

the results based on any of the four methods for reducing the moment data are not in good agreement with those based on the air loads. Consequently, a detailed inspection of these results is not warranted at this point. Some general observations can be made, however.

Tip deflections, rather than the generalized air loads, have been tabulated, since the physical significances of their relative magnitudes are more easily visualized. According to the results shown in Table IV based on the air-load measurements, the first-mode displacements dominate at the first three harmonics, and first and second modes dominate at the fourth and fifth harmonics. Deflection amplitudes are indicated to be small (less than 0.1 inch) for harmonics above the fifth.

Roughly, the tip deflections obtained from the air-load analysis and the bending-moment analyses follow similar trends. The results from the bending-moment calculations consistently show larger deflections than were calculated from the lift distributions for the fourth mode. The calculations made using the total deflection technique tend to indicate larger modal deflections than any of the other calculation methods for modes above the first in harmonics above the sixth.

Although tip deflections are easily visualized, they are not the fundamental quantities. It is of interest to convert them to the corresponding generalized air loads. These are presented in Table V. The same comparative trends exist as in the tip deflection data (Table IV); but the effect of the undamped amplification factor, $\frac{1}{(\omega_n^2 - k^2\Omega^2)\left(\frac{\overline{W}}{g}\right)_n}$, is to make the relatively small higher-mode tip deflections yield relatively large generalized forces. For example, using the tip deflections derived from air loads, the fourth-mode cosine deflection is less than 1% of the first-mode cosine deflection at the first harmonic, while the fourth-mode cosine generalized air load is 12% of the first-mode cosine generalized air load at the first harmonic.

TABLE V

COMPARISON OF DERIVED GENERALIZED AIR LOADS

Method of Analysis	Harmonic Order $k = \frac{\omega}{\Omega}$	GA_{1k} (pound) Cos	GA_{1k} (pound) Sin	GA_{2k} (pound) Cos	GA_{2k} (pound) Sin	GA_{3k} (pound) Cos	GA_{3k} (pound) Sin	GA_{4k} (pound) Cos	GA_{4k} (pound) Sin
Air Load		488.7	-507.7	-110.3	141.6	-148.1	139.7	62.0	14.4
Total Deflection		529.4	-478.4	4.3	-20.0	70.4	-28.5	438.6	-746.0
Single Mode	1	444.2	-502.9	-	-	-	-	-	-
Multi Mode		446.5	-513.2	-31.3	-32.0	-134.2	125.9	-112.4	46.7
Ortho Moments		436.5	-511.7	-30.8	-41.8	-133.5	127.0	-114.4	47.7
Air Load		-136.6	139.0	-92.6	-167.3	-40.6	-57.2	-73.9	35.5
Total Deflection		-143.2	89.5	-167.5	-177.1	-183.1	-23.3	-1094.0	-462.2
Single Mode	2	-90.3	103.6	-	-	-	-	-	-
Multi Mode		-102.7	98.4	-99.8	-89.8	42.5	16.8	265.8	21.5
Ortho Moments		-102.0	98.9	-101.5	-91.5	46.6	19.9	267.8	22.5
Air Load		42.8	-103.8	-30.6	10.2	-15.6	2.4	-19.4	-34.0
Total Deflection		43.7	-67.2	-77.6	-33.7	-106.4	-92.6	-262.6	-419.1
Single Mode	3	21.7	-71.4	-	-	-	-	-	-
Multi Mode		19.0	-71.5	-47.2	12.8	-39.4	21.9	-4.7	86.2
Ortho Moments		19.0	-71.6	-47.5	12.9	-39.1	22.2	-4.7	86.2
Air Load		47.5	-11.4	-21.0	-18.8	-12.5	14.8	-6.4	10.2
Total Deflection		75.5	-14.4	-31.5	-6.3	-91.1	66.7	-180.6	103.5
Single Mode	4	-	-	-27.7	-7.3	-	-	-	-
Multi Mode		56.8	9.7	-23.4	-3.6	-6.8	37.4	-17.2	47.2
Ortho Moments		57.2	10.9	-23.3	-3.9	-7.3	38.8	-18.1	47.2
Air Load		37.2	4.8	-3.1	8.2	-11.6	-1.1	4.7	-5.6
Total Deflection		14.5	9.6	-1.0	1.3	43.3	35.4	7.7	116.3
Single Mode	5	-	-	1.1	1.9	-	-	-	-
Multi Mode		121.6	18.9	0.8	1.9	15.9	-6.3	-12.0	2.6
Ortho Moments		121.8	19.3	0.8	1.9	15.4	-6.7	-12.3	2.6
Air Load		-1.3	37.3	-12.4	3.2	3.7	-21.8	3.0	-5.2
Total Deflection		-26.1	49.1	-21.0	21.5	30.2	-39.6	94.2	-136.5
Single Mode	6	-	-	12.4	5.8	-	-	-	-
Multi Mode		131.6	6.3	0.7	5.9	1.2	2.9	-16.6	-7.1
Ortho Moments		131.5	6.4	0.7	5.9	1.2	2.9	-16.6	-7.1
Air Load		13.0	1.9	-4.1	-2.3	-1.6	5.2	9.4	-0.5
Total Deflection		117.1	38.4	39.3	24.1	-12.6	-15.0	-70.1	-30.8
Single Mode	7	-	-	-	-	0.4	-8.3	-	-
Multi Mode		150.9	-74.1	2.8	4.8	2.4	-11.2	-10.0	-8.6
Ortho Moments		150.9	-73.3	2.9	4.8	2.4	-11.2	-10.7	-8.6
Air Load		-0.7	10.8	-1.7	3.5	-1.6	-0.5	-1.3	-4.6
Total Deflection		64.8	-142.9	21.1	-71.6	2.2	-3.6	-16.4	121.4
Single Mode	8	-	-	-	-	0.9	1.1	-	-
Multi Mode		125.7	-154.9	7.4	5.1	0.6	1.8	-13.2	-30.2
Ortho Moments		125.4	-153.6	7.6	15.4	0.6	1.8	-13.2	-30.2
Air Load		4.6	5.5	0.7	-5.2	-2.4	2.8	-2.6	-2.9
Total Deflection		-139.6	-59.4	-116.8	-18.7	-31.3	-3.7	105.6	40.3
Single Mode	9	-	-	-	-	5.6	9.5	-	-
Multi Mode		-32.6	-188.2	5.9	4.1	5.4	15.1	-0.5	-24.4
Ortho Moments		-32.6	-186.1	6.2	4.1	5.4	15.3	-0.5	-24.4
Air Load		-0.8	0.4	-0.4	3.2	-1.0	2.3	-0.7	0
Total Deflection		-35.9	221.8	-6.3	158.9	-3.7	72.1	-4.2	-72.3
Single Mode	10	-	-	-	-	-	-	7.4	0.4
Multi Mode		-256.4	-391.5	-9.4	24.3	6.7	30.9	7.6	-11.3
Ortho Moments		-255.6	-385.1	-9.4	21.9	6.4	31.6	7.6	-11.8

A comparison of generalized air loads deduced from measured lift distributions with generalized air loads obtained from measured moment distributions should be significant, provided the differences are not lost in the measurement errors. Unfortunately, this appears to be the case with the available data, and a definitive comparison of the various moment reduction techniques cannot be made. This is demonstrated by a plausible, albeit imprecise, analysis of the air load and moment data presented in the next section.

4. ACCURACY REQUIREMENTS ON MEASUREMENT OF BENDING MOMENTS

The numerical results presented in the previous section failed to indicate consistent differences among the results that would permit the definitive evaluation of the various methods for analyzing the bending-moment measurement data. It was postulated that these differences might have been lost in the inaccuracies of the basic measurements of both the air loads and the moments. The manner in which this possibility was investigated is described in this section and proceeded as follows:

1. An estimate was made of the threshold and accuracy of the measured lift distributions presented in part (b) of Table II and of the generalized air loads derived from them.

2. The theoretical maximum bending moment per unit generalized air load in each mode and at each frequency was determined. These quantities multiplied by the appropriate values obtained in Step 1 constituted the errors in the bending moments that would be consistent with the estimated errors in the measured lift distributions.

3. The requirements derived in Step 2 on the threshold and accuracy of bending-moment measurements were compared with estimates of the corresponding quantities in the actual moment data as presented in part (a) of Table II.

4. On the basis of Step 3, an assessment was made of the validity of an evaluation of analysis techniques which depends upon the available data.

THRESHOLD AND ACCURACY OF GENERALIZED AIR LOADS CALCULATED FROM MEASURED LIFT DISTRIBUTIONS

The lift distributions presented in References 12 and 14 were obtained by integrating measured pressure distributions. On the basis of the discussions in these references, the accuracy of the lift distributions can be expected to be, at best, within $\pm$ 2% of full scale. It is (optimistically) assumed that the probable error is constant (independent of radial and azimuthal position) and equal to $\pm$ 0.2 pound per inch. This value is only about 2% of maximum measured lift at the inboard radial station. Finally these estimates must be interpreted in terms of probable errors in harmonic content at each radial station. It can be shown that the corresponding error and threshold for each harmonic component of the lift are both equal to $\pm$ 0.1 pound per inch. The scale of Figure 1 is such that the abscissa lines have thicknesses corresponding to the threshold and the circles drawn about the data points have radii equivalent to about 0.1 pound per inch. It is evident from Figure 1 that the air-load distributions at harmonics beyond the fifth are not well defined for this case [see part (c) of Table II].

Estimation of the accuracy and the threshold values of the generalized air loads requires an assumption about the manner in which the lift distribution errors are distributed with respect to the particular mode shapes considered. For the purposes of the present discussion it is assumed that the lift errors are distributed in such a way that the generalized air-load error is maximized. This conservatism is at least partly compensated for by the optimistic assumptions regarding the accuracy of the lift distributions.

The maximum error in the generalized air load is given by

$$\Delta(G.A.)_{nk} = \pm \int_{r_o}^{R} |\mathcal{E}_k||\phi_n| dr$$

where

$\mathcal{E}_k$ = error in the k^{th} harmonic component of the air load measurement at each radial station, pounds per inch

ϕ_n = value of the normalized mode-shape deflection for the n^{th} mode.

Similarly, the maximum threshold generalized air load is given by

$$\delta(G.A)_{nk} = \pm \int_{r_o}^{R} |\Lambda_k||\phi_n| dr$$

where

Λ_k = threshold value of the k^{th} harmonic component of the air load measurement at each radial station, pounds per inch

The values obtained for these quantities were virtually independent of mode shape and were found to be

$$\Delta (G.A.)_n \approx \pm 12 \text{ pounds}$$

$$\delta (G.A.)_n \approx \pm 12 \text{ pounds}$$

based on the previously obtained values

$$\mathcal{E}_k \approx \pm 0.1 \text{ pound per inch}$$

$$\Lambda_k \approx \pm 0.1 \text{ pound per inch.}$$

A review of the generalized air loads presented in Table III in light of these possible errors shows that many of the tabulated values are probably highly inaccurate. This is demonstrated in Table VI, where all those values given in Table III which are less than the estimated threshold have been deleted as having no meaning (indicated by the shaded boxes) and where the possible percentage errors in the remaining values are as indicated. Almost all the generalized air loads for the harmonics above the fourth are less than the estimated threshold, and many of those indicated for the lower harmonics are subject to large errors. Table VI indicates that the evaluations of generalized air loads from the lift distributions are estimated to be in error by less than 100% for only the following cases: Mode 1: k = 1, 2, 3; Mode 2: k = 1, 2, 4; Mode 3: k = 1, 2, 4; and Mode 4: k = 1, 2, 3.

TABLE VI

ESTIMATED PERCENTAGE ERRORS IN THE GENERALIZED AIR LOADS EVALUATED FROM MEASURED PRESSURE DISTRIBUTIONS

Harmonic Order $\kappa = \omega/\Omega$		Mode 1 $\omega_1/\Omega = 2.72$	Mode 2 $\omega_2/\Omega = 4.95$	Mode 3 $\omega_3/\Omega = 7.84$	Mode 4 $\omega_4/\Omega = 13.1$
1	Cosine	2%	11%	8%	19%
	Sine	2%	8%	9%	83%
2	Cosine	9%	13%	30%	16%
	Sine	9%	7%	21%	34%
3	Cosine	28%	39%	77%	62%
	Sine	12%	-	-	35%
4	Cosine	25%	57%	96%	-
	Sine	-	64%	81%	-
5	Cosine	32%	-	-	-
	Sine	-	-	-	-
6	Cosine	-	96%	-	-
	Sine	32%	-	55%	-
7	Cosine	92%	-	-	-
	Sine	-	-	-	-
8	Cosine	-	-	-	-
	Sine	-	-	-	-
9	Cosine	-	-	-	-
	Sine	-	-	-	-
10	Cosine	-	-	-	-
	Sine	-	-	-	-

MAXIMUM MODAL BENDING MOMENT PER UNIT GENERALIZED AIR LOAD

The tip deflection (sine or cosine component) for a corresponding unit generalized air load is, from equation (7),

$$q_{nk} = \frac{1}{(\omega_n^2 - k^2\Omega^2)(\bar{w}/g)_n}$$

and the accompanying modal spanwise moment distribution is

$$M_{nk}(r) = q_{nk}\, m_n(r).$$

Since the maximum moment occurs at the station where the modal

moment per unit tip deflection is a maximum, $m_n(max)$, the above equations give the following expression for the maximum modal bending moment, $\hat{M}_{nk}$, for a unit generalized air load:

$$\hat{M}_{nk} = \frac{m_n(max)}{(\omega_n^2 - k^2\Omega^2)(\overline{W}/g)_n} \tag{26}$$

Values corresponding to equation (26) are given in Table VII.

TABLE VII
MAXIMUM MODAL MOMENTS FOR UNIT GENERALIZED AIR LOADS

Harmonic Order $K = \frac{\omega}{\Omega}$	$\hat{M}_{nk}$ for Unit Generalized Air Load, inch-pounds			
	Mode 1 $\frac{\omega_1}{\Omega} = 2.72$	Mode 2 $\frac{\omega_2}{\Omega} = 4.96$	Mode 3 $\frac{\omega_3}{\Omega} = 7.84$	Mode 4 $\frac{\omega_4}{\Omega} = 13.1$
1	5.51	5.71	5.21	2.89
2	10.39	6.54	5.49	2.95
3	21.90	8.65	6.00	3.04
4	4.09	15.72	6.93	3.17
5	2.00	304.0	6.64	3.37
6	1.23	11.75	12.38	3.64
7	0.85	5.50	25.34	4.02
8	0.62	3.41	122.3	4.58
9	0.48	2.38	16.09	5.43
10	0.38	1.28	8.16	6.85

BENDING-MOMENT MEASUREMENT ACCURACIES CORRESPONDING TO LIFT DISTRIBUTION ACCURACIES

The accuracy and threshold values required from bending-moment measurements to obtain generalized air loads to the same accuracy as those obtained from the lift distributions can now be estimated. The appropriate equations are

$$\Delta M(n,k) = \hat{M}_{nk}\left[\Delta(G.A.)_n\right] \tag{27}$$

$$\delta M(n,k) = \hat{M}_{nk}\left[\delta(G.A.)_n\right] . \tag{28}$$

The threshold value is calculated whenever the generalized air load in Table III is less than δ (G.A.). 12 pounds. Results are shown in Table VIII.

TABLE VIII
BENDING-MOMENT MEASUREMENT ACCURACY
CORRESPONDING TO LIFT DISTRIBUTION ACCURACY

Harmonic Order		Required Bending Moment Accuracy, inch-pounds			
		Mode 1	Mode 2	Mode 3	Mode 4
$K = \omega/\Omega$		ω_1/Ω = 2.72	ω_2/Ω = 4.96	ω_3/Ω = 7.84	ω_4/Ω = 13.1
1	Cosine	±66	±68	±63	±35
	Sine	±66	±68	±63	±35
2	Cosine	±125	±78	±66	±35
	Sine	±125	±78	±66	±35
3	Cosine	±263	±104	±72	±37
	Sine	±263	±104	±72	±37
4	Cosine	±49	±189	±83	±38
	Sine	±49	±189	±83	±38
5	Cosine	±24	±3650	±104	±41
	Sine	±24	±3650	±104	±41
6	Cosine	±15	±141	±149	±44
	Sine	±15	±141	±149	±44
7	Cosine	±10	±66	±304	±48
	Sine	±10	±66	±304	±48
8	Cosine	±7	±41	±1470	±55
	Sine	±7	±41	±1470	±55
9	Cosine	±6	±28	±193	±65
	Sine	±6	±28	±193	±65
10	Cosine	±5	±15	±98	±82
	Sine	±5	±15	±98	±82

Table VIII indicates the accuracy and threshold requirements on the measurement of bending moments if the generalized air loads are expected to be determined with an accuracy of ± 12 pounds and a threshold of ±12 pounds. The numbers enclosed in shaded boxes correspond to values within the threshold. Note, again, that the moment values apply at the station at which the particular mode has its maximum value and that greater accuracy would be required at all other stations.

At this point it should be recalled that the preceding arguments in this section were biased to reduce the requirements on bending-moment accuracy. The maximum estimated error was used with respect to obtaining generalized air loads from the pressure distribution measurements, and the maximum mode moment was used in estimating moment measurement requirements.

THRESHOLD AND ACCURACY OF THE BENDING-MOMENT MEASUREMENTS

As indicated in the data presented in part (a) of Table II, the oscillatory bending moments for the flight condition investigated ranged from -336 inch-pounds $\leq M \leq$ 3495 inch-pounds at $\frac{r}{R}$ = 0.15 to -6942 $\leq M \leq$ 5097 at $\frac{r}{R}$ = 0.65. A range of ±4000 inch-pounds is taken for purposes of this discussion. The accuracy is estimated to be 3% and the threshold approximately 1% of the reference value. These give an estimated accuracy of ±120 inch-pounds and a threshold of ±40 inch-pounds.

ACCURACY OF GENERALIZED AIR LOADS OBTAINED FROM BENDING-MOMENT MEASUREMENTS

A comparison of the bending-moment measurement accuracies estimated above with the requirements presented in Table VIII shows that the generalized air loads could be derived from the bending moments with an accuracy at least as good as from the lift distribution for only the following points:

Mode 1: k = 2, 3
Mode 2: k = 3, 4, 5, 6
Mode 3: k = 5, 6, 7, 8, 9
Mode 4: None

Only at these points can the bending-moment data be considered as good as the lift distribution. An evaluation of the various methods of analyzing the bending moment by comparison with results

based on the lift distribution is, therefore, possible, at most, at the above points. It was shown previously, however, that the generalized air loads can be derived from the lift distributions with reasonable accuracy at only certain of these points. Consequently, a valid comparison is possible at only the following conditions:

Mode 1: k = 2, 3
Mode 2: k = 4
Mode 3: None
Mode 4: None

Even of these, the expected accuracies of the reference generalized air loads for the first mode, third harmonic and the second mode, fourth harmonic are not very good (see Table VI). A definitive judgment of the analysis methods cannot be made on the basis of the extremely small sample that remains. The results presented in Tables III and IV are, therefore, not indicative of the relative merits of the various analysis techniques since the manner in which the data were reduced was not based on considerations of the validity of the measurements.

The whole discussion of accuracy was predicated on the assumption that the blade natural frequencies were known without error. This assumption could not be tested in the present program. Note that the ability to detect higher harmonic air loads from bending moments depends strongly on the amplification of the bending response near resonance. Errors in natural frequency determination could, therefore, degrade the results.

Finally, it is apparent that at least an order of magnitude improvement in bending-moment measurements is necessary if approximate generalized air loads are to be obtained up to the eighth harmonic. It is probable that such an improvement cannot be obtained without the development of specialized filtering and recording equipment.

5. GENERALIZED AIR LOADS, GENERALIZED FORCES, AND AIR-LOAD DISTRIBUTIONS

The analysis techniques discussed thus far in this report have been concerned with the reduction of either air-load measurements or bending-moment measurements to modal tip deflections or, what is equivalent, to "generalized air loads." Without the introduction of any assumptions relative to the air-load distribution, the generalized air load constitutes the only possible interface for comparing results based on the two different measurements. Recall, however, that the generalized air load is the integral over the span of the product of the n^{th} mode shape times the lift distribution at the k^{th} harmonic and includes the lift components due to bending slope and bending velocity. As a consequence of this dependence on the blade's elastic deformation, the generalized air load does not provide the blade designer with the basic information which he can extrapolate to the analysis of other, even geometrically similar, blades. Neither the air-load measurements nor the bending-moment measurements can, by themselves, fulfill this need, regardless of the analysis procedures. Therefore, the concept of the "generalized force" (References 1, 2, and 5), in which the damping, intermodal, and interharmonic aerodynamic force coefficients are assumed known, was introduced. It was postulated that the generalized forces for one rotor blade together with the assumed motion-dependent loads might then be used to estimate the effects of the air loads on other rotor blades, provided they are structurally and geometrically similar. The relationship between generalized air load and generalized force can be seen in the following development.

In the terminology of equation (1), the spanwise distribution of aerodynamic loading is approximated by

$$\ell\left(r,t,\frac{\partial y}{\partial r},\frac{\partial y}{\partial t}\right) \cong t_a(r,t) - a_o \frac{\rho}{2} c(r)\left(\Omega r + V\sin\Omega t\right)\left(\frac{\partial y}{\partial t} + V\frac{\partial y}{\partial r}\cos\Omega t\right) \quad (29)$$

where $t_a(r,t)$ is the aerodynamic loading that depends only on radius, r, and time, t, (i.e., independent of blade response), and the last term is the aerodynamic component that depends on blade bending velocity and bending slope. As in Section 1, the bending deflection is represented by

$$y(r,t) = \sum_{n=1}^{\infty} \phi_n(r) \sum_{k=0}^{\infty} \left(q_{nk_c} \cos k\Omega t + q_{nk_s} \sin k\Omega t \right) \tag{30}$$

and the aerodynamic loading $t_a(r,t)$ is given by

$$t_a(r,t) = \sum_{k=0}^{\infty} \left(t_{a_{k_c}} \cos k\Omega t + t_{a_{k_s}} \sin k\Omega t \right). \tag{31}$$

Again, the principle of virtual work is invoked and the orthogonality condition on the natural bending mode shapes is used so that, finally, the equation expressing the equilibrium of transverse forces takes the form derived in Reference 5:

$$\begin{aligned}
\sum_{k=0}^{\infty} \Bigg\{ & \left(\omega_m^2 - k^2\Omega^2\right)\left(\frac{\bar{W}}{g}\right)_{n_1} q_{mk_c} \cos k\Omega t \\
& + \frac{a_0 \rho}{4} \sum_{n=1}^{\infty} \Bigg[\frac{1}{2} V^2{}_2 C_{H_{mn}} q_{nk_s} \left(\cos(k-2)\Omega t - \cos(k+2)\Omega t \right) \\
& + \Omega V_1 C_{H_{mn}} q_{nk_c} \left(\cos(k+1)\Omega t + \cos(k-1)\Omega t \right) \\
& - \Omega V k_1 C_{M_{mn}} q_{nk_c} \left(\cos(k-1)\Omega t - \cos(k+1)\Omega t \right) \\
& + 2k\Omega^2{}_0 C_{M_{mn}} q_{nk_s} \cos k\Omega t \Bigg] \Bigg\} \\
& = \sum_{k=0}^{\infty} G_{mk_c} \cos k\Omega t
\end{aligned} \tag{32}$$

and

$$\sum_{k=0}^{\infty}\left\{\left(\omega_m^2 - k^2\Omega^2\right)\left(\frac{\bar{W}}{g}\right)_m q_{mk_s}\sin k\Omega t\right.$$

$$+\frac{a_0\rho}{4}\sum_{n=1}^{\infty}\left[\frac{1}{2}V^2{}_2C_{Hmn}\,q_{nk_s}\left(\sin(k+2)\Omega t - \sin(k-2)\Omega t\right)\right.$$

$$+\Omega V_1 C_{Hmn}\,q_{nk_c}\left(\sin(k+1)\Omega t + \sin(k-1)\Omega t\right)$$

$$-\Omega V k\,{}_1C_{Mmn}\,q_{nk_c}\left(\sin(k+1)\Omega t - \sin(k-1)\Omega t\right) \qquad (33)$$

$$\left.\left.+2k\Omega^2{}_0C_{Mmn}\,q_{nk_s}\sin k\Omega t\right]\right\}$$

$$=\sum_{k=0}^{\infty}G_{mk_s}\sin k\Omega t$$

where

$$\left(\frac{\bar{W}}{g}\right)_m \equiv \int_0^R m(r)\,\phi_m^2(r)\,dr$$

$${}_2C_{Hmn} \equiv \int_0^R c(r)\,\phi_m(r)\,\frac{d\phi_n(r)}{dr}\,dr$$

$${}_1C_{Hmn} \equiv \int_0^R rc(r)\,\phi_m(r)\,\frac{d\phi_n(r)}{dr}\,dr$$

$${}_1C_{Mmn} \equiv \int_0^R c(r)\,\phi_m(r)\,\phi_n(r)\,dr$$

$${}_0C_{Mmn} \equiv \int_0^R rc(r)\,\phi_m(r)\,\phi_n(r)\,dr \qquad (34)$$

$$G_{mk_c} \equiv \int_0^R t_{a_{k_c}}(r)\,\phi_m(r)\,dr$$

$$G_{mk_s} \equiv \int_0^R t_{a_{k_s}}(r)\,\phi_m(r)\,dr.$$

The generalized force, G_{mk} , is thus seen to be the integral over the span of the product of the m^{th} mode shape times the k^{th} harmonic of only that part of the aerodynamic loading which is independent of the blade deformation. The generalized force does not, therefore, represent the effect of the total load acting on the blade, and the estimate of the motion-dependent air loads must be introduced in both the evaluation of the generalized force from measured data and its application to another blade. The value of the concept of the generalized force is limited, therefore, by the error introduced in the approximation of that part of the air-load distribution.

In equations (32) and (33) for the cosine and sine components of the generalized force, those terms involving $C_{H_{mn}}$ and $C_{H'_{mn}}$ relate to intermodal coupling, and terms involving $k \pm 1$ or $k \pm 2$ are the interharmonic coupling effects. Even in this relatively complete representation, the unsteady aerodynamic effects have been approximated by quasi-steady aerodynamics, and the effects of reversed flow have been neglected. The intermodal and interharmonic aerodynamic coupling effects are neglected completely when the generalized force derives from the Single-Mode method of analyzing bending-moment measurement data.

The discussion above is in terms of the history of the generalized force idea. It was, in its time, a useful approach. It is reemphasized here, however, that the errors introduced through the assumptions with respect to the distribution, amplitude, and phasing of the motion-dependent forces have not been evaluated and, hence, the whole scheme must be used with caution. An insidious situation can develop. For example, generalized forces derived from data on one rotor and applied to another "similar" rotor could give perfect results (within the accuracy of the measurements) if the two were, in fact, aerodynamically and structurally identical and if the same assumed motion-dependent loads are used in both cases. But this same result would have been achieved by <u>any</u> arbitrary division of the loads

between motion-dependent and motion-independent components as long as the same division was observed in the reconstruction. The limits of applicability of schemes for deducing generalized forces from generalized air loads are not known, and experimental data to establish the required "similarity" are not available.

6. CONCLUDING REMARKS

1. Theoretically, no other set of basic functions can, with the same finite number of terms, fit the bending-moment measurements better than the orthonormal-moment distributions derived in this report.

2. "Generalized air loads" constitute the only interface for comparing analytical procedures based on bending-moment measurements and air-load distribution measurements.

3. Accuracy and threshold limits on available bending-moment and pressure measurements preclude the definitive evaluation of the various methods of analyzing moment data and, therefore, the practical verification of Item 1, above.

4. Neither the bending-moment measurements nor the air-load distribution measurements are sufficient in themselves to provide (without assumptions relative to the motion-dependent aerodynamics) a semiempirical method for estimating blade exciting forces for design purposes.

5. Whether bending-moment measurements or air-load distribution measurements comprise the basis for the evaluation of the generalized air loads, additional knowledge of the deformation-dependent part of the air loads is required in order to then derive the generalized forces.

7. RECOMMENDATIONS

1. It is recommended that a method be developed for evaluation of the motion-dependent aerodynamic forces by using all the experimental information available (lift distributions, blade root motions, and moment distributions).

All the following recommendations are contingent on the success of Item 1.

2. An estimate of the relative importance of sources of errors should be obtained. To this end, it is recommended that a numerical experiment be conducted. Blade structural characteristics and air loads could be postulated and used to determine moment distributions, natural frequencies, root slopes, etc. These generated data then could be treated as errorless measurements from which air-load distributions could be deduced. Comparison of these deduced loads with those originally specified would furnish a measure of the accuracies obtained with different reduction techniques (i. e., bases), dimensions (number of modes), etc. Further, the generated data could be perturbed with known errors and an estimate could be made of the manner in which these propagate. An effort should be made to interpret the findings of the error study in terms of (1) the accuracy with which natural frequencies, mode shapes, and bending moments must be known and (2) preferred gage locations.

3. Development of specialized filtering equipment is recommended if it is the decision of USAAVLABS to utilize one (or more) of the reduction techniques discussed in this report. The purpose of this equipment would be the improvement of measurement accuracy. This could be done, for example, by the introduction of properly phased and accurately

calibrated signals to extract most of the zeroth, first, and second harmonic components from the gage signals. The resulting net signals then could be amplified to display higher harmonic signal contents with standard recording equipment. Use of the device in model tests and prototype flight tests would enhance the structural data obtained.

4. An exploratory study of the use of edgewise strain measurements to construct drag-load distributions is recommended. The initial effort should be devoted to obtaining estimates of measurement accuracy requirements.

5. An exploratory study of the feasibility of including flapwise-edgewise-torsional coupling effects is recommended. Such effects might not be important with respect to interpretation of helicopter rotor structural moment distributions, but they could be important to the interpretation of data obtained on highly twisted propellers.

REFERENCES

1. Daughaday, H., and Kline, J., Cornell Aeronautical Laboratory, Inc., H-5 Variable Stiffness Blade Program: Part 6: A Tentative Empirical Criterion for the Design of Rotor Blades for Higher Mode Resonances, Wright Air Development Center, Dayton, Ohio, WADC Report AFTR6329 Part 6, November 1952.

2. Daughaday, H., and Kline, J., An Approach to the Determination of Higher Harmonic Rotor Blade Stresses, Cornell Aeronautical Laboratory, Buffalo, New York, CAL Report 52, March 1953.

3. Caseria, R., and Marlott, W., Conversion of Blade Bending Moment Measurements to Blade Deflections, Sikorsky Helicopter Corporation, Stratford, Connecticut, Sikorsky Report No. SER-50053, October 24, 1958.

4. Piziali, R. A., and DuWaldt, F. A., Cornell Aeronautical Laboratory, Inc., A Method for Computing Rotary Wing Airload Distribution in Forward Flight, U. S. Army Transportation Research Command,* Fort Eustis, Virginia, TCREC Technical Report 62-44, November 1962.

5. Loewy, R. G., Sternfeld, H., Jr., and Spencer, R. H., Vertol Division Boeing Company, Evaluation of Rotor Blade Generalized Exciting Forces as Determined from Flight Strain Data, Wright Air Development Division, Dayton, Ohio, WADD Report TR 59-24, February 1960.

6. Hirsch, H., and Kline, J., Cornell Aeronautical Laboratory, Inc., H-5 Variable Stiffness Blade Program: Part 1: Harmonic Reduction of Measured Blade Beam Bending Moment Data, Wright Air Development Center, Dayton, Ohio, WADC Report AFTR 6329, Part 1, December 1951.

7. Hirsch, H., and Kline, J., Cornell Aeronautical Laboratory, Inc., H-5 Variable Stiffness Blade Program: Part 2: Blade Beam Bending Envelopes, Wright Air Development Center, Dayton, Ohio, WADC Report AFTR 6329, Part 2, January 1952.

8. Hirsch, H., and Kline, J., Cornell Aeronautical Laboratory, Inc., H-5 Variable Stiffness Blade Program: Part 3: Evaluation of Rotor Blade Resonant Bending Effects, Wright Air Development Center, Dayton, Ohio, WADC Report AFTR 6329, Part 3, January 1952.

*Now U. S. Army Aviation Materiel Laboratories

9. Kline, J., Cornell Aeronautical Laboratory, Inc., H-5 Variable Stiffness Blade Program: Part 4: Harmonic Reduction of Measured Blade Motion and Control Force Data, Wright Air Development Center, Dayton, Ohio, WADC Report AFTR 6329, Part 4, April 1952.

10. Kline, J., Cornell Aeronautical Laboratory, Inc., H-5 Variable Stiffness Blade Program: Part 5: Evaluation of Blade Beam Bending Data Measured by Three Helicopter Manufacturers, Wright Air Development Center, Dayton, Ohio, WADC Report AFTR 6329, Part 5, June 1952.

11. Indrity, J., Methods in Analysis, The Macmillan Company, New York, New York, 1963, pp. 15-19.

12. Scheiman, J., A Tabulation of Helicopter Rotor-Blade Differential Pressures, Stresses, and Motions as Measured in Flight, National Aeronautics and Space Administration, Washington, D. C., NASA Technical Memorandum TM X-952, March 1964.

13. Targoff, W. P., Cornell Aeronautical Laboratory, Inc., The Bending Vibrations of a Twisted Rotating Beam, Wright Air Development Center, Dayton, Ohio, WADC Report TR 56-27, December 1955.

14. Burpo, F. B., and Lynn, R. R., Bell Helicopter Company, Measurement of Dynamic Air Loads on A Full-Scale Semirigid Rotor, U. S. Army Transportation Research Command, Fort Eustis, Virginia, TCREC Technical Report 62-42, December 1962.

DISTRIBUTION

US Army Materiel Command	5
US Army Mobility Command	3
US Army Aviation Materiel Command	5
US Army Aviation Materiel Laboratories	28
US Army Limited War Laboratory	1
US Army Human Engineering Laboratories	1
US Army Research Office-Durham	1
US Army Test and Evaluation Command	1
Plastics Technical Evaluation Center	1
US Army Medical R&D Command	1
US Army Engineer Waterways Experiment Station	1
US Army Combat Developments Command, Fort Belvoir	2
US Army Combat Developments Command Experimentation Command	3
US Army Command and General Staff College	1
US Army Aviation School	1
US Army Infantry Center	2
US Army Tank-Automotive Center	2
US Army Aviation Maintenance Center	2
US Army Electronics Command	2
US Army Aviation Test Activity, Edwards AFB	2
Air Force Flight Test Center, Edwards AFB	2
US Army Field Office, AFSC, Andrews AFB	1
Air Force Flight Dynamics Laboratory, Wright-Patterson AFB	1
Systems Engineering Group (RTD), Wright-Patterson AFB	3
Air Proving Ground Center, Eglin AFB	1
Bureau of Ships, DN	1
Bureau of Naval Weapons, DN	6
Chief of Naval Research	4
David Taylor Model Basin	1
Testing and Development Division, US Coast Guard	1
Ames Research Center, NASA	1
Lewis Research Center, NASA	1
Manned Spacecraft Center, NASA	1
NASA Representative, Scientific and Technical Information Facility	2
Research Analysis Corporation	1
NAFEC Library (FAA)	2
National Tillage Machinery Laboratory	1
US Army Board for Aviation Accident Research	1
Bureau of Safety, Civil Aeronautics Board	2
US Army Aviation Human Research Unit	2

US Naval Aviation Safety Center, Norfolk	1
Federal Aviation Agency, Washington, D.C.	2
The Surgeon General	1
Defense Documentation Center	20

UNCLASSIFIED

Security Classification

DOCUMENT CONTROL DATA - R&D

(Security classification of title, body of abstract and indexing annotation must be entered when the overall report is classified)

1 ORIGINATING ACTIVITY *(Corporate author)*

Cornell Aeronautical Laboratory, Inc.
Buffalo, New York 14221

2a. REPORT SECURITY CLASSIFICATION

UNCLASSIFIED

2b GROUP

3. REPORT TITLE

Derivation of Rotor Blade Generalized Air Loads From Measured Flapwise Bending Moment and Measured Pressure Distributions

4. DESCRIPTIVE NOTES *(Type of report and inclusive dates)*

Final Report - June 1964 through September 1965.

5. AUTHOR(S) *(Last name, first name, initial)*

DuWaldt, Frank A.

Statler, Irving C.

6. REPORT DATE	7a. TOTAL NO. OF PAGES	7b. NO. OF REFS
March 1966	50	14

8a. CONTRACT OR GRANT NO.	9a. ORIGINATOR'S REPORT NUMBER(S)
DA 44-177-AMC-198(T)	USAAVLABS Technical Report 66-13
b. PROJECT NO. 1P125901A14229	
c.	9b. OTHER REPORT NO(S) *(Any other numbers that may be assigned this report)*
d.	CB-1959-S-1

10. AVAILABILITY/LIMITATION NOTICES

Distribution of this document is unlimited.

11. SUPPLEMENTARY NOTES	12. SPONSORING MILITARY ACTIVITY
	U.S. Army Aviation Materiel Laboratories, Ft. Eustis, Virginia 23604

13. ABSTRACT

A limited study of method of deducing generalized air loads acting on a helicopter rotor blade or a propeller blade from bending-moment measurements is presented. A new set of basic functions called "orthonormal-moment distributions" is proposed as the best set for fitting the moment data.

DD FORM 1 JAN 64 1473

UNCLASSIFIED

Security Classification

14. KEY WORDS	LINK A		LINK B		LINK C	
	ROLE	WT	ROLE	WT	ROLE	WT

INSTRUCTIONS

1. ORIGINATING ACTIVITY: Enter the name and address of the contractor, subcontractor, grantee, Department of Defense activity or other organization *(corporate author)* issuing the report.

2a. REPORT SECURITY CLASSIFICATION: Enter the overall security classification of the report. Indicate whether "Restricted Data" is included. Marking is to be in accordance with appropriate security regulations.

2b. GROUP: Automatic downgrading is specified in DoD Directive 5200.10 and Armed Forces Industrial Manual. Enter the group number. Also, when applicable, show that optional markings have been used for Group 3 and Group 4 as authorized.

3. REPORT TITLE: Enter the complete report title in all capital letters. Titles in all cases should be unclassified. If a meaningful title cannot be selected without classification, show title classification in all capitals in parenthesis immediately following the title.

4. DESCRIPTIVE NOTES: If appropriate, enter the type of report, e.g., interim, progress, summary, annual, or final. Give the inclusive dates when a specific reporting period is covered.

5. AUTHOR(S): Enter the name(s) of author(s) as shown on or in the report. Enter last name, first name, middle initial. If military, show rank and branch of service. The name of the principal author is an absolute minimum requirement.

6. REPORT DATE: Enter the date of the report as day, month, year; or month, year. If more than one date appears on the report, use date of publication.

7a. TOTAL NUMBER OF PAGES: The total page count should follow normal pagination procedures, i.e., enter the number of pages containing information.

7b. NUMBER OF REFERENCES: Enter the total number of references cited in the report.

8a. CONTRACT OR GRANT NUMBER: If appropriate, enter the applicable number of the contract or grant under which the report was written.

8b, 8c, & 8d. PROJECT NUMBER: Enter the appropriate military department identification, such as project number, subproject number, system numbers, task number, etc.

9a. ORIGINATOR'S REPORT NUMBER(S): Enter the official report number by which the document will be identified and controlled by the originating activity. This number must be unique to this report.

9b. OTHER REPORT NUMBER(S): If the report has been assigned any other report numbers *(either by the originator or by the sponsor)*, also enter this number(s).

10. AVAILABILITY/LIMITATION NOTICES. Enter any limitations on further dissemination of the report, other than those imposed by security classification, using standard statements such as:

(1) "Qualified requesters may obtain copies of this report from DDC."

(2) "Foreign announcement and dissemination of this report by DDC is not authorized."

(3) "U. S. Government agencies may obtain copies of this report directly from DDC. Other qualified DDC users shall request through _____."

(4) "U. S. military agencies may obtain copies of this report directly from DDC. Other qualified users shall request through _____."

(5) "All distribution of this report is controlled. Qualified DDC users shall request through _____."

If the report has been furnished to the Office of Technical Services, Department of Commerce, for sale to the public, indicate this fact and enter the price, if known.

11. SUPPLEMENTARY NOTES: Use for additional explanatory notes.

12. SPONSORING MILITARY ACTIVITY: Enter the name of the departmental project office or laboratory sponsoring *(paying for)* the research and development. Include address.

13 ABSTRACT. Enter an abstract giving a brief and factual summary of the document indicative of the report, even though it may also appear elsewhere in the body of the technical report. If additional space is required, a continuation sheet shall be attached.

It is highly desirable that the abstract of classified reports be unclassified. Each paragraph of the abstract shall end with an indication of the military security classification of the information in the paragraph, represented as *(TS), (S), (C), or (U).*

There is no limitation on the length of the abstra t. However, the suggested length is from 150 to 225 words.

14. KEY WORDS. Key words are technically meaningful terms or short phrases that characterize a report and may be used as index entries for cataloging the report. Key words must be selected so that no security classification is required. Identifiers, such as equipment model designation, trade name, military project code name, geographic location, may be used as key words but will be followed by an indication of technical context. The assignment of links, rules, and weights is optional.